

Grafting of nano-silica onto ramie fiber for enhanced mechanical and interfacial properties of ramie/epoxy composite*

Anna DILFI K. F.^{1,2,3}, Zi-jin CHE^{1,2,3}, Gui-jun XIAN^{†‡1,2,3}

¹Key Lab of Structures Dynamic Behavior and Control of the Ministry of Education, Harbin Institute of Technology, Harbin 150090, China

²Key Lab of Smart Prevention and Mitigation of Civil Engineering Disasters of the Ministry of Industry and Information Technology, Harbin Institute of Technology, Harbin 150090, China

³School of Civil Engineering, Harbin Institute of Technology, Harbin 150090, China

[†]E-mail: gjxian@hit.edu.cn

Received May 14, 2019; Revision accepted July 29, 2019; Crosschecked Aug. 6, 2019

Abstract: To enhance the bonding properties between ramie fiber and epoxy resin, the ramie fiber was modified using nano-silica grafting. Hydrophilic nano-silica treated with water-soluble sodium dodecyl sulfate (SDS) and organic silane coupling agents was grafted onto the surface of ramie fiber. The surface roughness of the fibers was considerably increased after grafting. The nano-silica particles on the fiber surface enhanced the mechanical and thermal properties of the fiber-epoxy composite plates. Based on an analysis of contact angle measurements and a water absorption study, it was determined that the hydrophilicity of the treated fiber was weakened.

Key words: Nano-silica; Sodium dodecyl sulfate (SDS); Silane coupling agent; Ramie fiber; Mechanical properties; Interfacial properties

<https://doi.org/10.1631/jzus.A1900186>

CLC number: TQ31

1 Introduction

Natural fibers are widely used in polymer composites as reinforcements because of their advantages compared to synthetic fibers such as low cost, high specific modulus, biodegradability, good corrosion resistance, heat insulation, and regeneration (John and Thomas, 2008; Zhu et al., 2009; Shih et al., 2010; Zhang et al., 2010). However, their inferior mechanical properties and limited processability to those of synthetic fibers are two drawbacks that hinder their use in high-end applications (Shah, 2013). Among plant fibers, ramie fiber has many advantages such as

a lower density and higher tensile strength compared to that of flax and jute; moreover, its tensile strength is comparable to that of glass fiber (Yu et al., 2010). This fiber has been investigated as a reinforcement with various polymer matrices, namely, polylactic acid, epoxy, polyester, and polypropylene (Chen et al., 2011; Feng et al., 2011; Gu et al., 2014).

The properties of fiber-reinforced composites depend on the properties of the constituent components, the characteristic of the interfacial bonds, the adhesion between the fiber and matrix, and the load transfer mechanism at the interface (Kuzmin et al., 2017). Given that these fibers are hydrophilic, their adhesion with a hydrophobic matrix is not sufficient to provide a significant improvement in the mechanical properties of the composite. Heterogeneities of the fiber's surface such as surface defects, impurities, and surface flaws significantly affect the mechanical properties of the composites. Modification of the fiber's surface is generally utilized to reduce surface

[‡] Corresponding author

* Project supported by the Chinese MIIT Special Research Plan on Civil Aircraft (No. MJ-2015-H-G-103) and the National Natural Science Foundation of China (No. 51878223)

 ORCID: Gui-jun XIAN, <https://orcid.org/0000-0002-8540-2580>

© Zhejiang University and Springer-Verlag GmbH Germany, part of Springer Nature 2019

defects and improve the adhesion between the fiber and the matrix, resulting in an improvement of the mechanical properties of the composites (Varga et al., 2010). The addition of nanofillers is an efficient method for improving the mechanical properties and the interfacial adhesion given that the presence of the fiber and nanoparticles generate a multi-scale, multifunctional reinforcement in the composite system (Fan et al., 2008). A multi-scale reinforcement system containing fibers together with nano-scale particles in a matrix or on the fiber's surface has been determined to increase the delamination resistance of the polymer composite (Warrier et al., 2010; Gao et al., 2011; Jia et al., 2013).

Silica is one of the most abundant materials on the Earth's surface. It has been used in a wide variety of applications, such as glass, electronic devices, and nanotech devices (Fogarty et al., 2010; Yeon and van Duin, 2016). Silica particles as reinforcement in a polymer composite system reduce polymer shrinkage upon curing, increase thermal conductivity and mechanical properties, and decrease the thermal expansion coefficients. It is expected that the addition of nano-silica to a composite system would lead to a significant improvement in the physicomechanical properties of the composite such as the elastic modulus and thermal stability. However, the presence of abundant hydroxyl groups on the silica surface results in severe agglomeration of the silica particles and makes it hydrophilic. Thus, the affinity towards hydrophobic matrices is also significantly reduced. It has been reported that the surface modification of hydrophilic inorganic materials improves the compatibility between the filler and the hydrophobic organic polymer matrices (Abbasian et al., 2019; Linec and Music, 2019). The use of organic modifiers such as silane and alkanolic acids is a common method for modification of the surface of nano-silica to exhibit hydrophobic behavior. The agglomeration of hydrophilic particles that limits the rate of diffusion is a disadvantage in this case (Aissaoui et al., 2012; Li et al., 2013b).

Hsieh et al. (2008) indicated that nano-sized silica-coated onto carbon fiber fabrics induces remarkable enhancing effects such as the enhancement of the static contact angle. Vashisth and Bakis (2019) investigated the effects of nano-silica on the properties of carbon fiber composites produced via the fil-

ament winding process. The results indicated that the longitudinal and transverse compressive strength of the carbon/epoxy material increased significantly with the addition of nano-silica. In the case of carbon fiber/epoxy laminates, the incorporation of nano-silica was reported to be very effective in enhancing the interlaminar toughness (Zeng et al., 2012). Although these studies are related to carbon fibers, the positive results imply that it is possible to develop a modification method using nano-sized silica for natural fiber-based composites.

In the present study, woven ramie fibers were grafted with nano-sized silica and the treated fibers were then saturated with an epoxy resin to form composite plates. The modification of nano-silica was performed using sodium dodecyl sulfate (SDS), 3-aminopropyltrimethoxy silane (APS), and 3-glycidoxypropyltrimethoxysilane (GPS). The ramie fiber/epoxy interface was modified by incorporating modified hydrophobic nano-silica particles onto the fiber's surface. The composite plates containing the multi-scale, multifunctional reinforcements were fabricated via a vacuum assisted resin infusion (VARI) molding technique. The effect of the modified ramie fiber with nano-silica on the mechanical and interfacial properties of the ramie/epoxy composite was investigated.

2 Experimental

2.1 Raw materials and sample preparation

Commercial nano-silica particles (Boyu Gaoke New Material Technology Co. Ltd., Beijing, China) with an average particle size of 12 nm and a specific surface area of (200 ± 25) m²/g were used. SDS (Tianli Chemical Reagent Co. Ltd., Tianjin, China), APS (Guangzhou Zhongjie Chemical Technology Co. Ltd., Guangzhou, China), and GPS (Chengong Silicon Company, Nanjing, China) were used to treat nano-silica. The reinforcing micro filler used in the study was woven ramie fiber (Beijing Institute of Aeronautical Materials, Beijing, China) with an area density of 140 g/m². The epoxy used was the diglycidyl ether of bisphenol-F (DGEBF) (Nanya Plastic Corporation, Taipei, China). The epoxide equivalent was 163.8 g/eq and the density was 1.19 g/cm³. Methyl hexahydrophthalic anhydride (MHHPA)

(Qingyang Chemistry Co., Ltd., Jiaxing, China) was used as the curing agent and ethanol (Tianli Chemical Reagent Co. Ltd., Tianjin, China) was used as a dispersing medium for silane coupling agents in the study.

2.2 Modification of nano-silica and surface treatment of ramie fiber

One-step modification of nano-silica with SDS and surface treatment of ramie fiber were performed in an aqueous phase while the modification of nano-silica using silane coupling agents (APS and GPS) and surface treatment of the ramie fiber was performed in an organic medium. The medium used for dispersion and modification of nano-silica was a solution of SDS in water and silane coupling agents in ethanol. The concentrations of SDS, APS, and GPS were fixed at 1% in the dispersion. Nano-silica particles were mixed with SDS in water (1:10) and ultrasonicated at (50 ± 2) °C for 15 min. The solution was kept at room temperature for 3 h to improve the dispersion. For surface modification of nano-silica, APS was ultrasonicated (80 W, 20 °C) in ethanol (APS:ethanol=1:10) for 30 min. Then, nano-silica was added to the silane solution and sonicated for 15 min. A series of stable dispersions with 0.5% and 1% (in weight) concentrations of nano-silica was prepared and used for fiber treatment. A similar process was repeated to modify the surface of nano-silica with GPS.

Prior to fiber treatment, the woven ramie fiber was washed with distilled water for 2 h under ultrasonication to remove dirt and waxy materials from the surface. The fiber was dried at 60 °C for 24 h in a hot air oven. The dried ramie fiber was then ultrasonicated in each nano-silica dispersion for 15 min and the in situ modified nano-silica was grafted onto the ramie fiber then dried at 60 °C for 24 h in a hot air oven.

2.3 Characterization of the nano-silica grafted fiber

1. Scanning electron microscope (SEM)

An SEM (Merlin compact with Gemini-I electron column, Zeiss Pvt. Ltd., Germany) was used to examine the fiber surfaces. The fibers cut from the fabric were gold-coated for 15 min via sputter coating (Gatan Model 682 Precision Etching Coating System, USA) SEM analysis.

2. Atomic force microscope (AFM)

The surface roughness of the treated fibers was investigated using a Bruker Dimension Icon AFM (California, USA) operated in tapping mode. Silicon AFM probes were used. Three points were investigated for each specimen on a $5\ \mu\text{m}\times 5\ \mu\text{m}$ surface area.

3. X-ray photoelectron spectroscopy (XPS)

To determine the elemental composition of the surface of the fiber and to confirm that the nano-silica is grafted onto the ramie fiber, X-ray photoelectron spectroscopy was conducted using a PHI 5700 ESCA system (Physical Electronics Co. Ltd., USA) equipped with an Al K α radiation source operating at 1486.6 eV. The pass energy from the wide scan to the narrow scan was 187.85 eV to 23.50 eV.

4. Fourier transform infrared (FTIR)

FTIR spectra of the fiber specimens (untreated and treated) were acquired using a spectrometer (Spectrum 100, Perkin Elmer Instruments, USA) operating in the range of 4000–400 cm^{-1} . The ramie fiber samples were converted to a powdered form and spectra were acquired using KBr as the matrix.

5. Contact angle measurement

Sessile drop experiments were conducted to analyze the wetting behavior of both the untreated and treated fibers at room temperature. The experiment was conducted using a goniometer (DropMeter™ Element A-60, MAIST Vision Inc., China) and the effect of fiber modification by nano-silica on the fiber water wettability was analyzed experimentally. The contact angle was obtained at the intersection between the fluid and the fiber surface. The experimental set up consisted of a high-resolution telecentric lens and a telecentric backlight illuminator coupled to a halogen light source. A single fiber was mounted horizontally on a sample stage and a water droplet was deposited on its surface. Image acquisition and the determination of the contact angle were performed using the Dropmeter software. More than ten readings were averaged to obtain the contact angle for each sample.

2.4 Fabrication and evaluation of the properties of the composite plate

The composite plates were prepared using a vacuum-assisted resin infusion (VARI) process as illustrated in Fig. 1. Tensile, flexural, and interfacial shear tests were performed according to ASTM

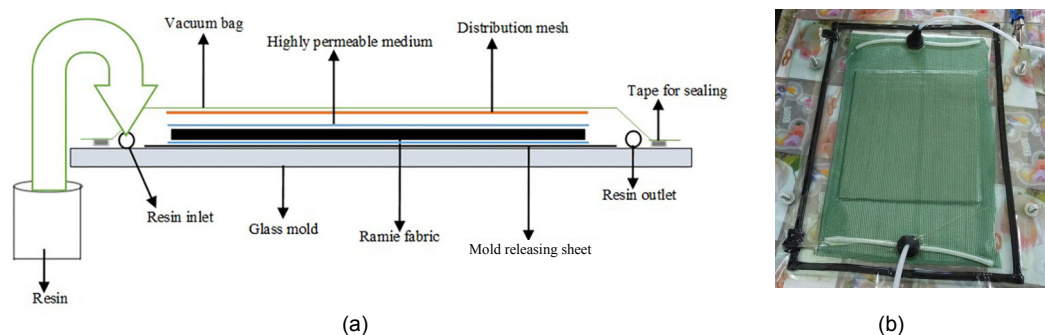


Fig. 1 Schematic (a) and digital image (b) of the VARI process

(2017), ASTM (2003), and ASTM (2016), respectively. Dynamic mechanical analysis (DMA) was performed using a DMA Q800 dynamic mechanical analyzer (TA Instruments, USA). The extent of water absorption of the specimens was investigated according to ASTM (2018). Detailed information related to the sample preparation process and testing is available in our previous studies (Dilfi K. F. et al., 2018, 2019).

Water absorption: The extent of water absorption of the specimens was investigated according to ASTM (2018). Rectangular specimens with dimensions described in ASTM were immersed in distilled water. The samples were then removed from the distilled water at regular time intervals, wiped with tissue paper to remove excess surface water, and weighed using an analytical balance with 0.1 mg accuracy. The samples were then re-immersed in the water to allow the sorption to continue until saturation was achieved.

3 Results and discussion

3.1 Mechanism for the grafting of nano-silica on the surface of the ramie fiber

In this study, a method for grafting modified nano-silica using water-soluble SDS and organic silane coupling agents and its effect on the mechanical and interfacial properties of ramie/epoxy composites were investigated. Given that SDS dissolves in water, the mixing of nano-silica in SDS results in improved dispersion and it effectively modifies the surface of nano-silica (Songolzadeh and Moghadasi, 2017). Based on subsequent analysis, the SDS

concentration, as well as the dispersion time and temperature were optimized. The optimum concentration of SDS was determined to be 1% (in weight). The temperature was controlled at (50 ± 2) °C and a dispersion time of 15 min was used. The conditions were maintained for 3 h to obtain a stable dispersion of the nano-silica. Due to the high surface energy and the presence of a large number of hydroxyl groups on the surface, nano-silica exhibits strong hydrophilicity and agglomeration and it minimizes the compatibility with the hydrophobic polymer matrix. When the agglomerated hydrophilic nano-silica treated with SDS and the silane coupling agents under ultrasonication, deagglomeration of nano-silica particles occurs and the surface is modified by the introduction of hydrophobic chains. Stable dispersions containing 0.5% and 1% (in weight) concentrations of nano-silica were prepared. The ramie fiber was ultrasonicated in each dispersion for 15 min and then dried in a hot air oven to produce nano-silica grafted ramie fiber. A schematic representation of the nano-silica modified via grafting on the ramie fiber using SDS and silane coupling agents subsequent to ultrasonication is illustrated in Fig. 2.

A reaction between the hydroxyl groups on the oxide surface and the modifier can occur (Wang et al., 2006). Bronsted acid sites on the silica surface can provide protons for the reaction between surface silanol groups and the modifier (Liu et al., 2015). SDS undergoes hydrolysis to form dodecanol and sodium hydrogen sulfate at the determined temperature (Fig. 3a). Dodecanol then reacts with the Bronsted acid sites on the nano-silica surface to form a carbocation. The carbocation reacts with the Si-O moiety to form Si-O-C structures (Fig. 3b) that exhibit

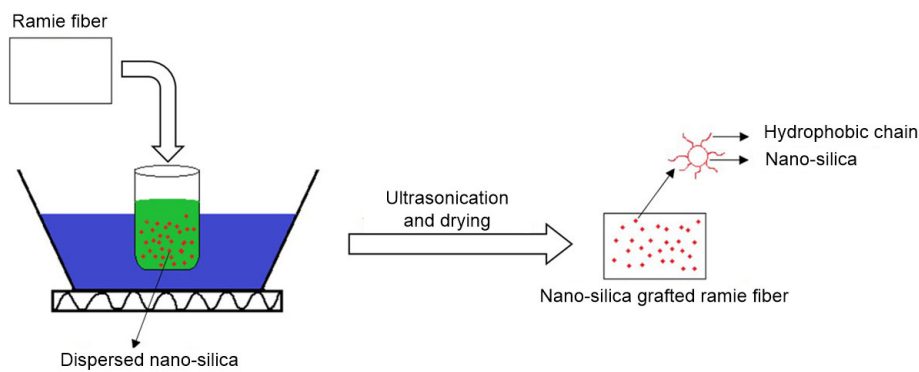


Fig. 2 Schematic of nano-silica modified via grafting on the ramie fiber

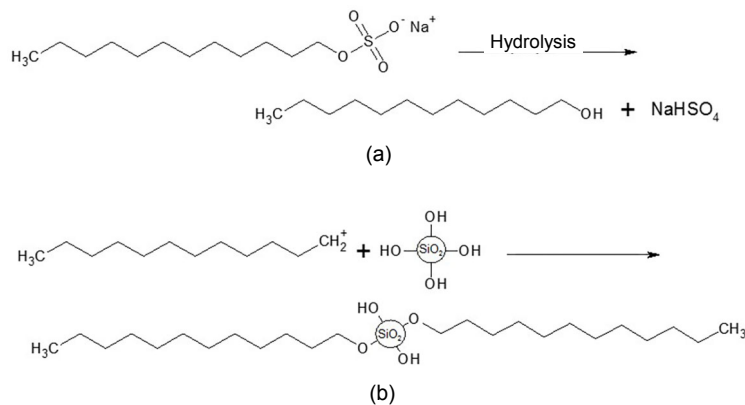


Fig. 3 Reaction mechanism of hydrolysis of SDS (a) and reaction between carbocation and silanol (b)

hydrophobicity (Li et al., 2013a; Khung et al., 2014). The modified surface reduces the hydrophilicity on the surface of the nano-silica thereby facilitating wetting and absorption of the hydrophobic polymer matrix. Hydroxyl groups on the nano-silica surface react with $-\text{OH}$ groups on the cellulose of the ramie fiber to form $\text{Si}-\text{O}-\text{C}$ covalent linkages between the nano-silica and ramie fiber.

Due to their unique bifunctional nature, silane coupling agents can be used to modify the surface of nano-silica. Surface treatment is usually performed via the chemical reaction between the surface silanol groups and the silane coupling agents. One end of the silane coupling agent can react with the silanol groups of nano-silica and the other end with the fiber. In the present study, two types of silane coupling agents, i.e. APS and GPS, were used. When silane coupling agents are added to the ethanol:water mixture, hydrolysis of the alkoxy groups occurs to produce silanol (Fig. 4a). The silanol formed on the silane thus undergoes a condensation reaction with the hydroxyl

groups on the fiber's surface and the silanol on the nano-silica forms a crosslinked network structure (Fig. 4b). The NH_2 group of APS interacts with the $-\text{OH}$ groups on silica to form a polyaminosiloxane network containing more than two APS units. The peak observed in the FTIR spectrum at 1570 cm^{-1} that is attributed to the deformation mode of the amino group in APS to form a hydrogen bond with silanol, confirms this observation. The grafting of surface-modified nano-silica particles onto the ramie fiber introduces nano-scale surface roughness (Wei et al., 2011). Schematic representations of the ramie fiber treated with SDS/nano-silica, APS/nano-silica, and GPS/nano-silica are shown in Fig. 5. It is worth noting that the grafting mechanism is similar to the grafting of nano-sized titanium dioxide (Wang et al., 2015).

3.2 Characterization of nano-silica grafted fiber

To characterize the surface morphology and roughness of the untreated and nano-silica grafted ramie fiber, an SEM analysis was conducted. SEM

images of the ramie fiber with the nano-hybrid coating are shown in Fig. 6. The images of the ramie fiber

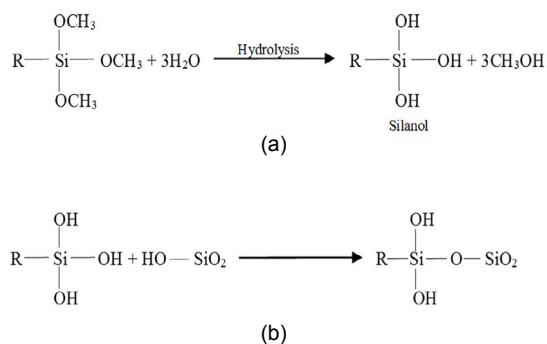


Fig. 4 Reaction mechanism of hydrolysis of silane (a), reaction between silane and nano-silica (b) (note: R=NH₂(CH₂)₃ for APS and R=(CH₂OCH)₂CH₂O(CH₂)₃ for GPS)

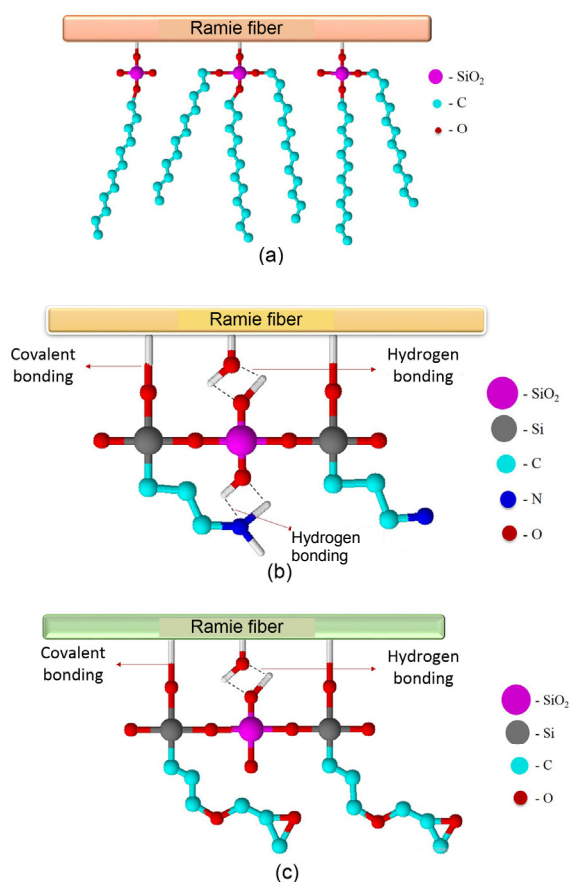


Fig. 5 Schematic of nano-silica grafted ramie fiber of SDS/nano-silica (a), APS/nano-silica (b), and GPS/nano-silica (c)

treated with SDS/nano-silica (1%), APS/nano-silica (1%), and GPS/nano-silica (1%, in weight) depict the appearance of nano-silica on the fiber's surface compared to the untreated fiber. The nano-silica grafted fiber surface appeared to be uneven in the SEM image under high magnification. It is evident that the nano-silica particles were uniformly deposited on the fiber's surface and increased the surface roughness. The GPS/nano-silica fiber morphology exhibited more closely packed nanoparticles on the surface compared to the other two nano-silica grafted ramie fiber surfaces, according to higher magnification SEM images. In the following of the study, C means the control fibers without any treatment, and S0, A0, and G0 mean the fiber treated with SDS, APS, and GPS without nano-silica. In addition, S1, A1, and G1 indicate the fiber treatment with SDS, APS, and GPS and 0.5% nano-silica, respectively. Similarly, S2 means the fiber treated with SDS and 1% (in weight) nano-silica.

AFM is a versatile technique for the characterization of natural fibers. In the present study, the fiber surface roughness was analyzed via AFM. The surface roughness of ramie fiber without nano-silica was determined to be 58.6 nm whereas those of the nano-silica grafted ramie fibers yielded values of 60.6 nm (S2), 68.6 nm (A2), and 78.0 nm (G2). The increase in the surface roughness could be due to the presence of nano-silica particles on the fiber's surface. A clear distinction in the surface topography could also be observed between the images of the nano-silica grafted ramie fiber compared to the untreated fiber surface.

XPS analysis was used to investigate the surface chemistry of untreated and nano-silica grafted ramie fibers, in addition to the effectiveness of the nano-hybrid coating on the ramie fiber. The presence of nano-silica on the ramie fiber surface was confirmed by the Si2p peaks in the XPS spectra (Fig. 7). The elemental composition percentage of each fiber after various chemical treatments is shown in Table 1. Compared to the untreated ramie fiber, the APS and GPS treated fibers exhibited a low peak for Si2p in the XPS spectrum. This is due to the presence of Si that is bonded to the cellulose fiber via silane coupling agents. The percent of Si increased after grafting the nano-silica on the ramie fiber using SDS, APS, and GPS (Table 1). This observation confirms the

grafting of nano-silica onto the surface of the ramie fiber.

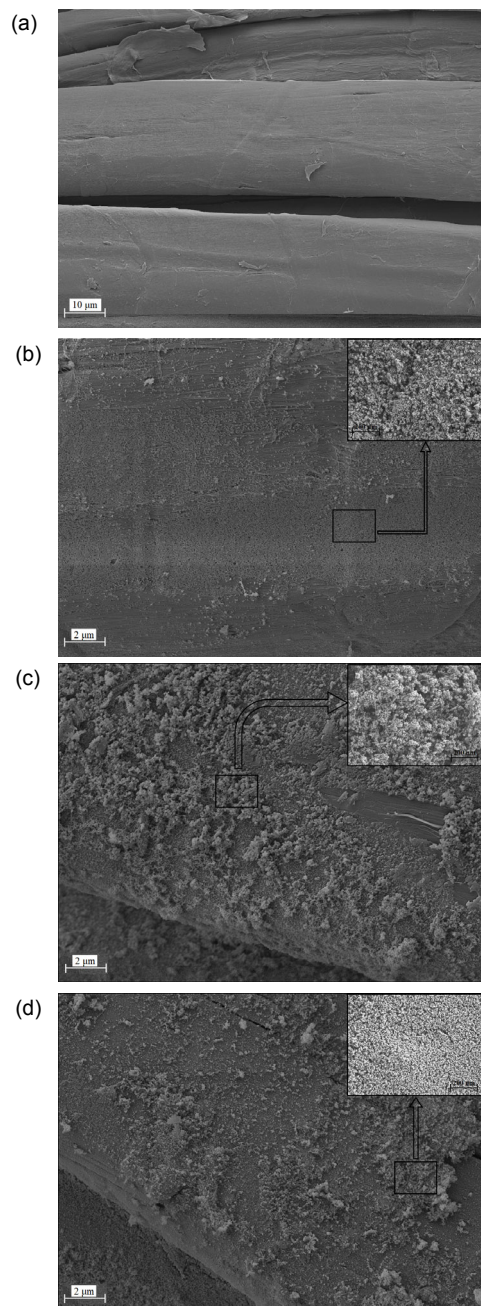


Fig. 6 SEM images of ramie fiber with and without nano-silica: C (a), S2 (b), A2 (c), and G2 (d)

Fig. 7 illustrates the FTIR spectra that explain the variation in the surface chemical structures of the untreated and nano-silica grafted ramie fibers. The wavenumber range and the bond characteristics of the peaks are given in Table 2.

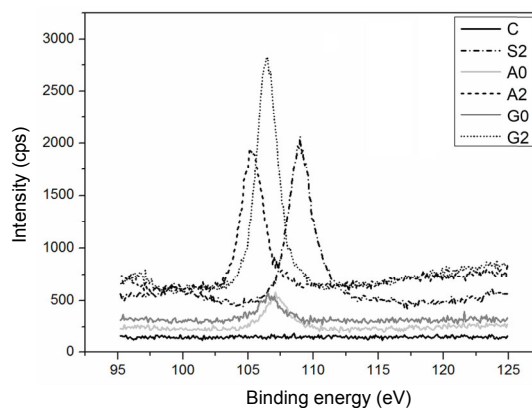


Fig. 7 Si2p peaks of ramie fiber with and without nano-silica

Table 1 Compositions of elements analyzed by XPS

| Sample | C1s (%) | O1s (%) | Si2p (%) |
|--------|---------|---------|----------|
| C | 69.47 | 30.53 | 0 |
| A0 | 78.37 | 17.03 | 2.99 |
| G0 | 69.55 | 28.54 | 1.90 |
| S2 | 47.42 | 38.91 | 12.23 |
| A2 | 53.71 | 20.96 | 14.50 |
| G2 | 52.84 | 21.24 | 14.33 |

By comparing the spectra of the untreated and nano-silica grafted ramie fiber, it is apparent that the base peaks of both spectra are the same. The peaks that correspond to nano-silica are observed in the short wavelength region in the spectra. In addition to the base peaks observed in the untreated ramie fiber, peaks at 698 cm^{-1} (SDS/nano-silica), 699 cm^{-1} (APS/nano-silica), and 704 cm^{-1} (GPS/nano-silica) were observed in the spectrum of the nano-silica grafted ramie fiber, which is indicative of overlapping of Si–C and Si–O stretching vibrations (Al-Oweini and El-Rassy, 2009). The characteristic peak of Si–O–Si observed at $470\text{--}420\text{ cm}^{-1}$ in the case of nano-silica grafted ramie fiber indicated the presence of SiO_2 (Kang et al., 2001). It is evident that the intensity of the peaks observed for the untreated fiber was reduced considerably. The peaks corresponding to the Si–O–C stretching vibrations were observed to overlap with the C–O–C asymmetric stretching vibrations at $1110\text{--}1050\text{ cm}^{-1}$. The peak observed at 1570 cm^{-1} in the APS/nano-silica corresponds to the deformation mode of the NH_2 group that forms hydrogen bonds with silanol (Kuzmin et al., 2017). The

peaks at 1300–900 cm^{-1} and 1500–1300 cm^{-1} are associated with C–O and C–H vibrations of cellulose. The peak at 2899 cm^{-1} is due to the CH_2 symmetric vibrations of cellulose. A broad band at 3500–3100 cm^{-1} due to the –OH functional group (free and hydrogen-bonded) was also observed in all the fibers.

Table 2 Peak positions and bond characteristics of ramie fiber with and without nano-silica

| C | Wavenumber range of peak (cm^{-1}) | | | Bond characteristics |
|-----------|---|------|------|---|
| | SDS | APS | GPS | |
| | 466 | 443 | 438 | Si–O–Si bending vibrations |
| | 702 | 702 | 708 | Si–O stretching vibrations |
| 1056 | 1056 | 1061 | 1061 | C–O–C asymmetrical stretching, C–C, C–OH, C–H ring and side group vibrations |
| 1112 | 1118 | 1112 | 1112 | C–O–C asymmetric stretching vibrations |
| 1320 | 1326 | 1326 | 1326 | CH_2 rocking vibration |
| 1433 | 1433 | 1433 | 1433 | C–OH in-plane vibration, CH_2 deformation vibration, NH_2 deformation |
| 1641 | | 1570 | | C=C stretching vibration |
| 2899 | 1658 | 1641 | 1641 | H–C–H symmetric stretching vibration |
| 3350–3450 | 2899 | 2899 | 2899 | –OH stretching vibration |

The properties of a polymer composite mainly depend on the adhesion characteristics between the reinforcement and the polymer matrix. The wetting measurement on a fiber yarn is an alternative method to analyze the adhesion characteristics (Hansen et al., 2017). A ‘drop-on-fiber yarn’ method was used in this study in which a water droplet was captured on the fiber yarn’s surface and the entire drop profile was measured via imaging. This information was used to obtain the contact angle. The water contact angle measurements also provide information about the hydrophilicity of the nano-silica grafted ramie fibers. However, it is widely recognized that the difference between advancing and receding contact angles plays an important role in determining hydrophobicity, compared to static contact angle measurements. Likewise, it is often very difficult to accurately determine the contact angles of natural fiber yarn. Some fibers protrude out from the fiber yarn which causes difficulty in determining the baseline of the water droplet.

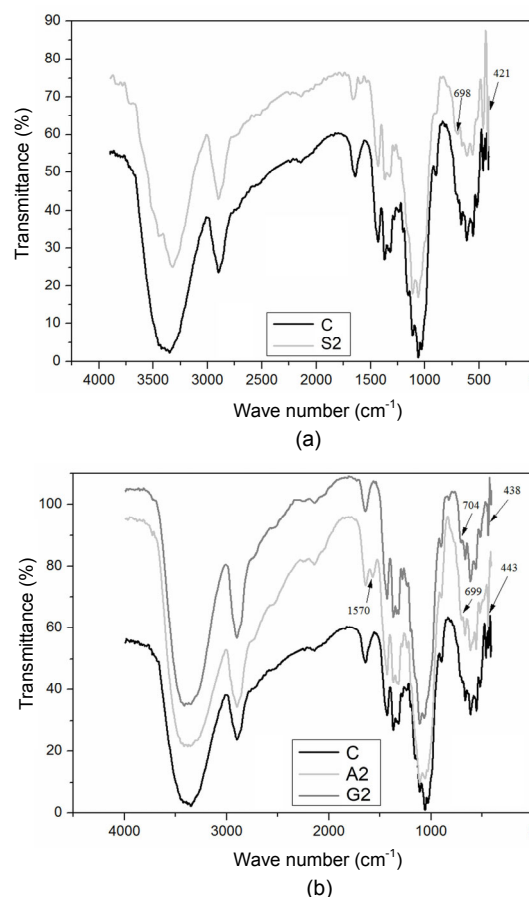


Fig. 8 Comparison of FTIR spectra of ramie fibers with and without nano-silica. (a) Untreated ramie fiber and SDS/nano-silica fiber; (b) Untreated ramie fiber, APS/nano-silica, and GPS/nano-silica fiber

In the present study, the water contact angles of untreated ramie fiber and the nano-silica grafted ramie fiber were compared. The water contact angles of each fiber were measured in a time period of 20 s after placing the water droplet on the surface of the fiber. The mean contact angle of the untreated and nano-silica grafted fibers are shown in Table 3. In the case of the former, a water contact angle of 31.2° was obtained whereas the nano-silica grafted ramie fiber had contact angles of 38.3° (SDS), 47.4° (APS), and 55.6° (GPS). The untreated ramie fiber was determined to have low water contact angle and was highly absorbent due to the abundance of hydroxyl groups in its molecular structure. The increase in the water contact angle of the nano-silica grafted ramie fiber implies that there was a reduction in the number of hydroxyl groups in the fiber’s molecular structure and the surface of the ramie fiber was successfully

modified by grafting with hydrophobic nano-silica (Hsieh et al., 2008). The dense nano-silica coating on the ramie fiber surface prevented the interaction between water molecules and the cellulosic fiber surface. Given that silica contains many silanol groups on its surface, it can be considered to be highly polar. Moreover, the surface hydroxyl groups tend to form hydrogen bonds with each other, resulting in strong filler-filler interactions and highly agglomerated silica particles. The ultrasonication of nano-silica with SDS and silane prevented the agglomeration of nano-silica and modified the surface via chemical grafting of SDS and silane on the nano-silica surface, resulting in a hydrophobic behavior. The grafting of hydrophobic nano-silica onto the surface of the ramie fiber under ultrasonication reduced the affinity of the fiber towards water. The modification of ramie fiber with hydrophobic nano-silica formed a strong and stable interface between the filler and the matrix.

Table 3 Mean contact angle values of ramie fiber with and without nano-silica

| Sample | Mean contact angle, θ ($^{\circ}$) | Sample | Mean contact angle, θ ($^{\circ}$) |
|--------|---|--------|---|
| C | 31.2 \pm 1.19 | A2 | 47.4 \pm 0.27 |
| S0 | 33.1 \pm 0.21 | G0 | 49.0 \pm 0.64 |
| S2 | 38.3 \pm 0.83 | G2 | 55.6 \pm 0.42 |
| A0 | 43.9 \pm 0.23 | | |

Note: data are presented as mean \pm standard deviation, $n=5$

3.3 Mechanical properties of the composite plate

The mechanical properties such as the tensile strength, flexural strength, and interfacial shear strength were examined to study the effect of nano-silica on the composites. There was a distinct improvement in the mechanical properties of the composites after the addition of nano-silica.

The tensile strength and elastic modulus are important mechanical properties of engineering materials. These two parameters of the composites with and without nano-silica are shown in Fig. 9. Compared to the composites without nano-silica, the tensile properties of the composites with nano-silica showed a significant improvement. This improvement gradually increases as the concentration of nano-silica increases. The percentage increase of the tensile strength and elastic modulus of composites with nano-silica is shown in Table 4. There was an

increase in the tensile strength of the composites with nano-silica (1%) of 10.87% (SDS), 19.20% (APS), and 20.06% (GPS). The elastic modulus exhibited 14.78% (SDS), 27.82% (APS), and 32.49% (GPS) increase with 1% (in weight) nano-silica grafting. The increase in tensile properties of the nano-silica grafted ramie fiber composite is attributed to the high stiffness of the nano-silica grafted on the ramie fiber, which modifies the fiber-matrix interface. The improvement in tensile properties is due to the effective interaction of hydrophobic nano-silica with the microfiber and the polymer matrix. The presence of hydrophobic nano-silica on the fiber's surface repairs the surface defects on the microfiber, which in turn delays crack opening (Siddiqui et al., 2010). In addition, the remarkable increase of the modulus may be attributed to more effective load sharing of the fibers between the treated fiber and the resin, as well as the possibility of an increase in the stiffness of the treated ramie fibers. A more detailed study on the mechanical properties of treated fibers is necessary to elucidate the related mechanisms.

The flexural strength and flexural modulus of the composites with and without nano-silica are shown in Fig. 10. The flexural properties of the fiber composites with nano-silica exhibited significant improvement compared to the composite without nano-silica. Table 5 shows the percentage increase in the flexural strength and modulus of the composites. It was observed that the composites grafted with 1% (in weight) nano-silica exhibited 20.53% (SDS), 25.72% (APS), and 32.88% (GPS) increase in the flexural strength and 63.52% (SDS), 64.64% (APS), and 71.34% (GPS) increase in the flexural modulus. It is well-known that the load applied to a composite is transferred to the filler via the interface. Therefore, a strong interface between the components of a composite is required for excellent properties. The increase in the flexural strength and the flexural modulus of the composites with nano-silica is attributed to the enhancement of the interfacial bonding between the microfiber and the matrix via the hydrophobic nano-silica. The large surface area of nano-silica contributes toward the improved adhesion between the microfiber and the polymer matrix. As a result, a good stress transfer from the matrix to the nano-filler and then to the microfiber occurs, which improves the flexural properties of the fiber composites modified with nano-silica.

The increase in the flexural modulus can also be related to the increase in the interfacial bonding of the composite (Sreekumar et al., 2009).

To better understand the mechanical properties in the interface region, ILSS (interlaminar shear strength) was evaluated for all the composites. When

the transverse shear load applied to a composite exceeds the ILSS, delamination failure occurs between the layers of reinforcing fibers. To induce interlaminar shear failure and to accurately measure the ILSS of a composite, a pure shear stress should be generated between the fiber layers. The short beam shear

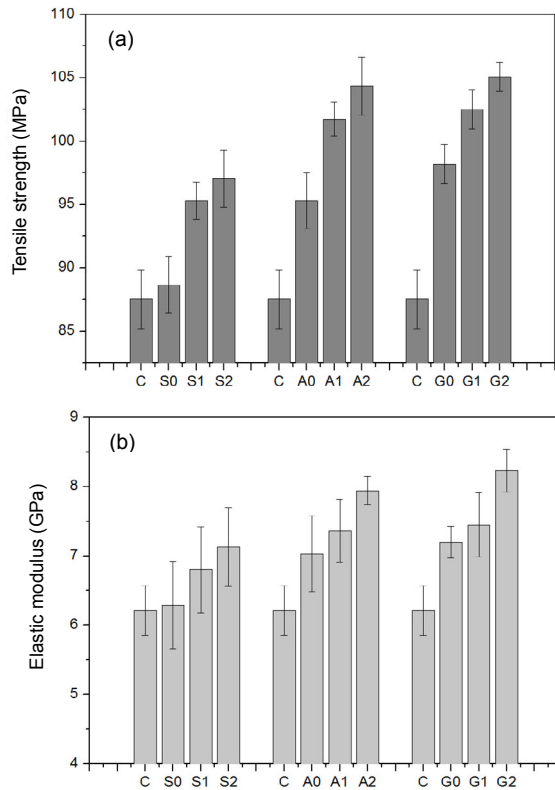


Fig. 9 Tensile strength (a) and elastic modulus (b) of composites with and without nano-silica

Table 4 Percentage increase in the tensile strength and elastic modulus of the composites with and without nano-silica

| Sample | Tensile strength increase (%) | Elastic modulus increase (%) |
|--------|-------------------------------|------------------------------|
| S0 | 1.27 | 1.26 |
| S1 | 8.88 | 9.47 |
| S2 | 10.87 | 14.78 |
| A0 | 8.88 | 13.17 |
| A1 | 16.24 | 18.54 |
| A2 | 19.20 | 27.82 |
| G0 | 12.20 | 15.91 |
| G1 | 17.09 | 19.93 |
| G2 | 20.06 | 32.49 |

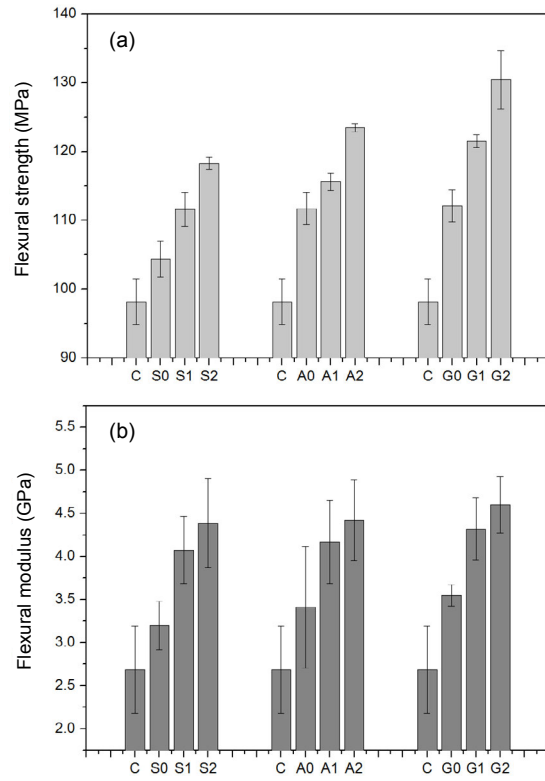


Fig. 10 Flexural strength (a) and flexural modulus (b) of composites with and without nano-silica

Table 5 Percentage increase in the flexural strength and flexural modulus of composites with and without nano-silica

| Sample | Flexural strength increase (%) | Flexural modulus increase (%) |
|--------|--------------------------------|-------------------------------|
| S0 | 6.32 | 19.22 |
| S1 | 13.67 | 51.82 |
| S2 | 20.53 | 63.52 |
| A0 | 13.80 | 27.02 |
| A1 | 17.77 | 55.32 |
| A2 | 25.72 | 64.64 |
| G0 | 14.20 | 32.23 |
| G1 | 23.81 | 60.88 |
| G2 | 32.88 | 71.34 |

method is the simplest approach among the available methods for determining the ILSS of the composites. As such, it is the most commonly used technique in practice. In this method, the specimen is loaded so that it fails during the interlaminar shear. The shear stress at failure is taken as the ILSS (Fan et al., 2008).

The ILSS of composites with and without nano-silica is presented in Fig. 11. It is observed that the addition of nano-silica to the composite system considerably enhances the ILSS and the maximum value is determined for the composite system containing 1% (in weight) nano-silica, which was approximately 12.09% (SDS), 17.34% (APS), and 18.70% (GPS) higher compared to the composite without nano-silica. This implies that the presence of hydrophobic nano-silica at the interface region of the composite system acts as an adhesion promoter between the microfiber and the polymer matrix. The absence of hydrophobic nano-silica as an adhesion promoter in the composite system containing the microfiber and the polymer matrix decreased the ILSS of the system. The stress transfer was effective at the interface region in the case of the microfiber modified with the hydrophobic nano-silica. The hydrophobic nano-silica on the microfiber surface absorbed the shear stress and efficiently transferred it to the fiber, which in turn improved the delamination failure in the interface region.

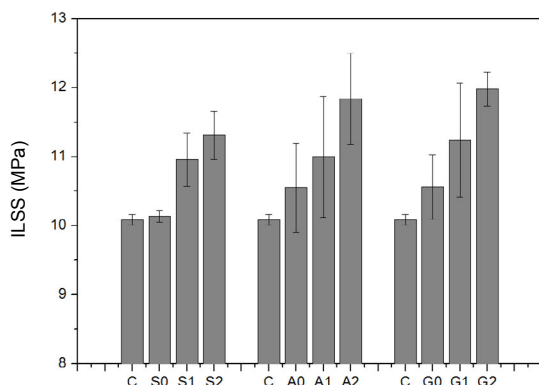


Fig. 11 Interlaminar shear strength of composites with and without nano-silica

The interfacial bond strength depends mainly on the characteristics or strength of the interaction between the constituent materials that comprise the interface region. In the case of the fiber composite without the nano-silica modification, the interfacial bond strength is weak. In the case of the fiber modi-

fied with nano-silica, the interfacial bond strength increases due to the effective bonding of hydrophobic nano-silica with the microfiber. As a result, the polymer matrix can completely wet the fiber's surface and significantly enhance the mechanical properties of the fiber composites modified by the hydrophobic nano-silica. The presence of nano-silica in the composite contributes to an increase in its stiffness, which results in an enhancement of the resistance against interlaminar failure, thereby increasing the elasticity of the composite.

3.4 Dynamic mechanical properties

DMA is an effective tool for determining the viscoelastic properties of composite materials. It provides information about the interfacial bonding of the reinforcing fiber and the polymer matrix of a composite material. The untreated and nano-silica grafted composites were subjected to DMA to analyze the damping behavior as a function of temperature. The storage moduli and $\tan\delta$ of the composites with and without nano-silica are shown in Fig. 12. All the composites exhibited a decrease in the storage modulus with the increase in temperature. At lower temperatures, the magnitude of the storage modulus of nano-silica grafted fiber composites showed a significant enhancement compared to the untreated fiber composites due to the greater transfer of interfacial stress. This is indicative of higher heat dissipation in composites with nano-silica grafted ramie fiber compared to composites without nano-silica. The observed results suggest that the composites with good interfacial adhesion dissipate less energy than the composites with poor interfacial bonding (Saba et al., 2016). The untreated ramie fiber has a weak adhesion to the epoxy matrix. As a result, the storage modulus of the untreated ramie fiber composite was determined to be less than that of the composites with the nano-silica grafted ramie fiber. The peak values of $\tan\delta$ of the composites with nano-silica grafted ramie fibers were reduced compared to that of the control sample, indicating a reduction of the damping factor. The interfacial bond strength was stronger in the nano-silica grafted ramie fiber composites compared to the untreated fiber composite. This was due to the improved adhesion between the fiber and the epoxy matrix as a result of the enhanced surface roughness and improved stiffness induced by the nanoparticles.

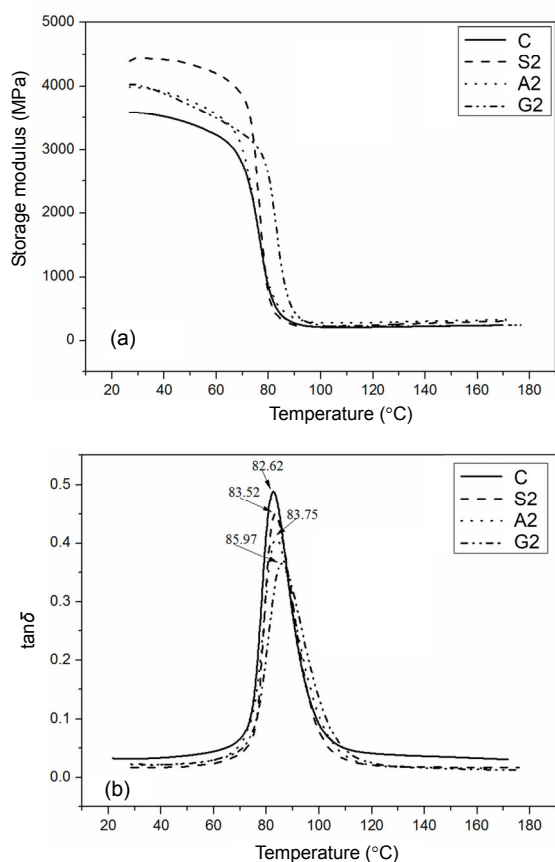


Fig. 12 Temperature dependence of storage modulus (a) and $\tan \delta$ of composites (b) with and without nano-silica

3.5 Effect of nano-silica on water absorption

The absorption of water can cause changes in the shape, debonding, or loss of strength in composites that are regularly exposed to moisture (Tserki et al., 2006). Fig. 13 depicts the effect of fiber modification using nano-silica on the water absorption characteristics of the ramie/epoxy composites. The purpose of fiber chemical modification is to reduce the hydrophilic characteristic of the fiber, thereby establishing a strong interface between the treated fiber and the hydrophobic polymer matrix. The chemically modified fiber composites exhibit a decreased rate of water absorption compared to the untreated fiber composite and the extent of water absorption varies depending on the nature of the chemical treatment. The fiber treated with silane coupling agents, APS/nano-silica, and GPS/nano-silica exhibited a lower rate of absorption than the fiber treated with SDS and SDS/nano-silica. This could be attributed to the enhanced fiber-matrix adhesion after modification. The

hydrophilicity of natural fibers is due to the abundance of the hydroxyl groups on the fiber cellulose structure. Upon chemical treatment with SDS, silane coupling agents, and nano-silica, the surface hydroxyl groups were reduced, thereby minimizing the hydrophilicity of the fiber. The silane coupling agents form strong chemical and hydrogen bonds that reduced the fiber-matrix debonding caused by moisture. It was observed that all the composites displayed less affinity towards water, which signifies that the fiber modification minimized the hydrophilic characteristic of the ramie fiber by favoring strong fiber-matrix interfacial adhesion.

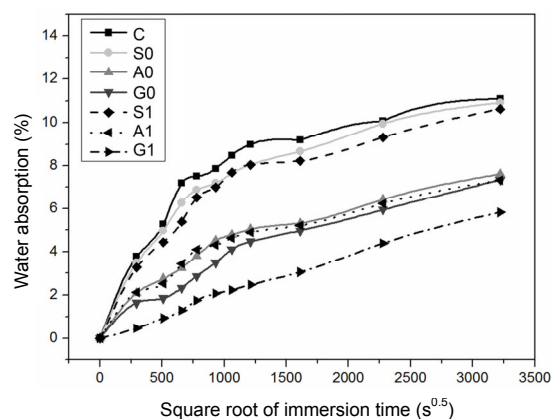


Fig. 13 Water absorption characteristics of composites with and without nano-silica

4 Conclusions

The surface of nano-silica was modified using water-soluble SDS and organic silane coupling agents. The modified nano-silica was grafted on the surface of ramie fiber and the effect of micro- and nano-fillers on the mechanical and interfacial properties were investigated. The following conclusions can be drawn from the present study.

The ramie fiber was grafted with modified nano-silica on the fiber's surface using SDS and silane coupling agents. The grafting process using GPS was determined to be more effective compared to other modifying methods.

The presence of nano-silica particles in SEM and AFM images, the characteristic peaks observed via FTIR analysis and the increase in the Si atomic weight percentage observed via XPS confirmed the

grafting of nano-silica on the surface of the ramie fiber.

The surface roughness of the fibers increased considerably after grafting nano-silica on its surface.

The hydrophilicity of the treated fiber was reduced by grafting nano-silica onto its surface. This was determined by an analysis of contact angle measurements and the water absorption study.

The nano-silica particles on the fiber's surface improved the bond strength between the fiber and epoxy matrix, which resulted in an enhancement of the mechanical and thermal properties of the composites.

Contributors

Anna DILFI K. F. wrote the first draft of the manuscript. Zi-jin CHE performed some tests. Gui-jun XIAN proposed the idea, supervised the research work, and revised and edited the final version.

Conflict of interest

Anna DILFI K.F., Zi-jin CHE, and Gui-jun XIAN declare that they have no conflict of interest.

References

- Abbasian M, Massoumi B, Mohammad-Rezaei R, et al., 2019. A novel epoxy-based resin nanocomposite: co-curing of epoxidized novolac and epoxidized poly(vinyl chloride) using amine-functionalized silica nanoparticles. *Materials Research Express*, 6:085346. <https://doi.org/10.1088/2053-1591/ab28c8>
- Aissaoui N, Bergaoui L, Landoulsi J, et al., 2012. Silane layers on silicon surfaces: mechanism of interaction, stability, and influence on protein adsorption. *Langmuir*, 28(1):656-665. <https://doi.org/10.1021/la2036778>
- Al-Oweini R, El-Rassy H, 2009. Synthesis and characterization by FTIR spectroscopy of silica aerogels prepared using several Si(OR)₄ and R''Si(OR')₃ precursors. *Journal of Molecular Structure*, 919(1-3):140-145. <https://doi.org/10.1016/j.molstruc.2008.08.025>
- ASTM, 2003. Standard Test Methods for Flexural Properties of Unreinforced and Reinforced Plastics and Electrical Insulating Materials, ASTM D790. American Society for Testing and Materials, West Conshohocken, USA.
- ASTM, 2016. Standard Test Method for Short-beam Strength of Polymer Matrix Composite Materials and Their Laminates, ASTM D2344. American Society for Testing and Materials, West Conshohocken, USA.
- ASTM, 2017. Standard Test Method for Tensile Properties of Polymer Matrix Composite Materials, ASTM D3039M. American Society for Testing and Materials, West Conshohocken, USA.
- ASTM, 2018. Standard Test Method for Water Absorption of Plastics, ASTM D570. American Society for Testing and Materials, West Conshohocken, USA.
- Chen DK, Li J, Ren J, 2011. Influence of fiber surface-treatment on interfacial property of poly(L-lactic acid)/ramie fabric biocomposites under UV-irradiation hydrothermal aging. *Materials Chemistry and Physics*, 126(3):524-531. <https://doi.org/10.1016/j.matchemphys.2011.01.035>
- Dilfi KF A, Balan A, Bin H, et al., 2018. Effect of surface modification of jute fiber on the mechanical properties and durability of jute fiber-reinforced epoxy composites. *Polymer Composites*, 39(S4):E2519-E2528. <https://doi.org/10.1002/pc.24817>
- Dilfi KF A, Che ZJ, Xian GJ, 2019. Grafting ramie fiber with carbon nanotube and its effect on the mechanical and interfacial properties of ramie/epoxy composites. *Journal of Natural Fibers*, 16(3):388-403. <https://doi.org/10.1080/15440478.2017.1423259>
- Fan ZH, Santare MH, Advani SG, 2008. Interlaminar shear strength of glass fiber reinforced epoxy composites enhanced with multi-walled carbon nanotubes. *Composites Part A: Applied Science and Manufacturing*, 39(3):540-554. <https://doi.org/10.1016/j.compositesa.2007.11.013>
- Feng YL, Hu YX, Zhao GY, et al., 2011. Preparation and mechanical properties of high-performance short ramie fiber-reinforced polypropylene composites. *Journal of Applied Polymer Science*, 122(3):1564-1571. <https://doi.org/10.1002/app.34281>
- Fogarty JC, Aktulga HM, Grama AY, et al., 2010. A reactive molecular dynamics simulation of the silica-water interface. *Journal of Chemical Physics*, 132(17):174704. <https://doi.org/10.1063/1.3407433>
- Gao X, Jensen RE, McKnight SH, et al., 2011. Effect of colloidal silica on the strength and energy absorption of glass fiber/epoxy interphases. *Composites Part A: Applied Science and Manufacturing*, 42(11):1738-1747. <https://doi.org/10.1016/j.compositesa.2011.07.029>
- Gu YZ, Tan XL, Yang ZJ, et al., 2014. Hot compaction and mechanical properties of ramie fabric/epoxy composite fabricated using vacuum assisted resin infusion molding. *Materials & Design*, 56:852-861. <https://doi.org/10.1016/j.matdes.2013.11.077>
- Hansen D, Bomholt N, Jeppesen JC, et al., 2017. Contact angle goniometry on single micron-scale fibers for composites. *Applied Surface Science*, 392:181-188. <https://doi.org/10.1016/j.apsusc.2016.09.018>
- Hsieh CT, Wu FL, Yang SY, 2008. Superhydrophobicity from composite nano/microstructures: carbon fabrics coated with silica nanoparticles. *Surface and Coatings Technology*, 202(24):6103-6108. <https://doi.org/10.1016/j.surfcoat.2008.07.006>
- Jia XL, Li G, Liu BY, et al., 2013. Multiscale reinforcement and interfacial strengthening on epoxy-based composites by silica nanoparticle-multiwalled carbon nanotube complex. *Composites Part A: Applied Science and Manufacturing*, 48:101-109. <https://doi.org/10.1016/j.compositesa.2013.01.001>
- John MJ, Thomas S, 2008. Biofibres and biocomposites.

- Carbohydrate Polymers*, 71(3):343-364.
<https://doi.org/10.1016/j.carbpol.2007.05.040>
- Kang S, Hong SI, Choe CR, et al., 2001. Preparation and characterization of epoxy composites filled with functionalized nanosilica particles obtained via sol-gel process. *Polymer*, 42(3):879-887.
[https://doi.org/10.1016/S0032-3861\(00\)00392-X](https://doi.org/10.1016/S0032-3861(00)00392-X)
- Khung YL, Ngalim SH, Meda L, et al., 2014. Preferential formation of Si-O-C over Si-C linkage upon thermal grafting on hydrogen-terminated silicon (111). *Chemistry: A European Journal*, 20(46):15151-15158.
<https://doi.org/10.1002/chem.201403014>
- Kuzmin KL, Timoshkin IA, Gutnikov SI, et al., 2017. Effect of silane/nano-silica on the mechanical properties of basalt fiber reinforced epoxy composites. *Composite Interfaces*, 24(1):13-34.
<https://doi.org/10.1080/09276440.2016.1182408>
- Li N, Hu P, Zhang XH, et al., 2013a. Effects of oxygen partial pressure and atomic oxygen on the microstructure of oxide scale of ZrB₂-SiC composites at 1500 °C. *Corrosion Science*, 73:44-53.
<https://doi.org/10.1016/j.corsci.2013.03.023>
- Li Y, Han BY, Liu L, et al., 2013b. Surface modification of silica by two-step method and properties of solution styrene butadiene rubber (SSBR) nanocomposites filled with modified silica. *Composites Science and Technology*, 88:69-75.
<https://doi.org/10.1016/j.compscitech.2013.08.029>
- Linec M, Music B, 2019. The effects of silica-based fillers on the properties of epoxy molding compounds. *Materials*, 12(11):1801-1811.
<https://doi.org/10.3390/ma12111811>
- Liu ZN, Xu KL, Sun H, et al., 2015. One-step synthesis of single-layer MnO₂ nanosheets with multi-role sodium dodecyl sulfate for high-performance pseudocapacitors. *Small*, 11(18):2182-2191.
<https://doi.org/10.1002/sml.201402222>
- Saba N, Jawaid M, Alothman OY, et al., 2016. A review on dynamic mechanical properties of natural fibre reinforced polymer composites. *Construction and Building Materials*, 106:149-159.
<https://doi.org/10.1016/j.conbuildmat.2015.12.075>
- Shah DU, 2013. Developing plant fibre composites for structural applications by optimising composite parameters: a critical review. *Journal of Materials Science*, 48(18):6083-6107.
<https://doi.org/10.1007/s10853-013-7458-7>
- Shih YF, Huang CC, Chen PW, 2010. Biodegradable green composites reinforced by the fiber recycling from disposable chopsticks. *Materials Science and Engineering: A*, 527(6):1516-1521.
<https://doi.org/10.1016/j.msea.2009.10.024>
- Siddiqui NA, Li EL, Sham ML, et al., 2010. Tensile strength of glass fibres with carbon nanotube-epoxy nanocomposite coating: effects of CNT morphology and dispersion state. *Composites Part A: Applied Science and Manufacturing*, 41(4):539-548.
<https://doi.org/10.1016/j.compositesa.2009.12.011>
- Songolzadeh R, Moghadasi J, 2017. Stabilizing silica nanoparticles in high saline water by using ionic surfactants for wettability alteration application. *Colloid and Polymer Science*, 295(1):145-155.
<https://doi.org/10.1007/s00396-016-3987-3>
- Sreekumar PA, Thomas SP, Saiter JM, et al., 2009. Effect of fiber surface modification on the mechanical and water absorption characteristics of sisal/polyester composites fabricated by resin transfer molding. *Composites Part A: Applied Science and Manufacturing*, 40(11):1777-1784.
<https://doi.org/10.1016/j.compositesa.2009.08.013>
- Tserki V, Matzinos P, Zafeiropoulos NE, et al., 2006. Development of biodegradable composites with treated and compatibilized lignocellulosic fibers. *Journal of Applied Polymer Science*, 100(6):4703-4710.
<https://doi.org/10.1002/app.23240>
- Varga C, Miskolczi N, Bartha L, et al., 2010. Improving the mechanical properties of glass-fibre-reinforced polyester composites by modification of fibre surface. *Materials & Design*, 31(1):185-193.
<https://doi.org/10.1016/j.matdes.2009.06.034>
- Vashisth A, Bakis CE, 2019. Multiscale characterization and modeling of nanosilica-reinforced filament wound carbon/epoxy composite. *Materials Performance and Characterization*, 8(1):1-21.
<https://doi.org/10.1520/mpc20180108>
- Wang HG, Xian GJ, Li H, 2015. Grafting of nano-TiO₂ onto flax fibers and the enhancement of the mechanical properties of the flax fiber and flax fiber/epoxy composite. *Composites Part A: Applied Science and Manufacturing*, 76:172-180.
<https://doi.org/10.1016/j.compositesa.2015.05.027>
- Wang ZW, Wang TJ, Wang ZW, et al., 2006. The adsorption and reaction of a titanate coupling reagent on the surfaces of different nanoparticles in supercritical CO₂. *Journal of Colloid and Interface Science*, 304(1):152-159.
<https://doi.org/10.1016/j.jcis.2006.08.039>
- Warrier A, Godara A, Rochez O, et al., 2010. The effect of adding carbon nanotubes to glass/epoxy composites in the fibre sizing and/or the matrix. *Composites Part A: Applied Science and Manufacturing*, 41(4):532-538.
<https://doi.org/10.1016/j.compositesa.2010.01.001>
- Wei B, Song SH, Cao HL, 2011. Strengthening of basalt fibers with nano-SiO₂-epoxy composite coating. *Materials & Design*, 32(8-9):4180-4186.
<https://doi.org/10.1016/j.matdes.2011.04.041>
- Yeon J, van Duin ACT, 2016. Reaxff molecular dynamics simulations of hydroxylation kinetics for amorphous and nano-silica structure, and its relations with atomic strain energy. *The Journal of Physical Chemistry C*, 120(1):305-317.
<https://doi.org/10.1021/acs.jpcc.5b09784>
- Yu T, Ren J, Li SM, et al., 2010. Effect of fiber surface-treatments on the properties of poly(lactic acid)/ramie composites. *Composites Part A: Applied Science and Manufacturing*, 41(4):499-505.
<https://doi.org/10.1016/j.compositesa.2009.12.006>
- Zeng Y, Liu HY, Mai YW, et al., 2012. Improving interlaminar

fracture toughness of carbon fibre/epoxy laminates by incorporation of nano-particles. *Composites Part B: Engineering*, 43(1):90-94.

<https://doi.org/10.1016/j.compositesb.2011.04.036>

Zhang HB, Zheng WG, Yan Q, et al., 2010. Electrically conductive polyethylene terephthalate/graphene nanocomposites prepared by melt compounding. *Polymer*, 51(5): 1191-1196.

<https://doi.org/10.1016/j.polymer.2010.01.027>

Zhu ZH, Imada T, Asakura T, 2009. Preparation and characterization of regenerated fiber from the aqueous solution of *Bombyx mori* cocoon silk fibroin. *Materials Chemistry and Physics*, 117(2-3):430-433.

<https://doi.org/10.1016/j.matchemphys.2009.06.028>



中文概要

题目: 苧麻表面接枝改性及其对苧麻纤维增强环氧复合材料力学性能与界面性能的影响研究

目的: 通过在苧麻纤维表面接枝纳米二氧化硅颗粒, 改善苧麻纤维与环氧树脂的界面粘结性能, 从而提高苧麻纤维增强环氧树脂复合材料的力学性能。

创新点: 将纳米二氧化硅颗粒接枝到苧麻纤维表面, 从而大幅提升苧麻纤维与环氧树脂的界面粘结性能与复合材料的力学性能。

方法: 利用十二烷基硫酸钠均匀分散二氧化硅纳米粒子, 并在硅烷偶联剂作用下, 将二氧化硅纳米粒子接枝到苧麻纤维表面。

结论: 纳米二氧化硅接枝到苧麻纤维表面大幅提升了纤维表面粗糙度, 降低了纤维亲水性能, 升高了纤维与环氧树脂的界面粘度, 从而改善了复合材料的力学性能。

关键词: 纳米二氧化硅; 十二烷基硫酸; 硅烷偶联剂; 苧麻纤维; 力学性能; 界面性能

Introducing Editorial Board Member:

Prof. Gui-jun XIAN has been an Editorial Board Member of *Journal of Zhejiang University-SCIENCE A (Applied Physics & Engineering)* since 2018.

Prof. XIAN obtained his PhD degree from Zhejiang University, China in 2001. Since then, he worked in the Institute of Composite Materials (IVW), Kaiserslautern University, Germany (2001–2005), and University of California, San Diego, USA (2005–2009). In 2009, Prof. XIAN joined the School of Civil Engineering, Harbin Institute of Technology (HIT), China. His research interests focus on novel fiber reinforced polymer composites and structures. By now, he has published more than 140 technical papers in international journals and conferences.

Prof. XIAN has been a member in the International Institute for FRP in Construction (IIFC) and the Society for the Advancement of Material and Process Engineering (SAMPE) of China. He is active in major international conferences related to FRP composites and structures. He was the co-chair of the 6th Asia-Pacific Conference on FRP in Structures (APFIS) and has given three international conference presentations as a keynote speaker in 2019.